Field-Induced Supersolid Phase in Spin-One Heisenberg Models

P. Sengupta[1,2] and C. D. Batista[1]

[1]*Theoretical Division, Los Alamos National Laboratory, Los Alamos, New Mexico 87545, USA*
[2]*MST-NHMFL, Los Alamos National Laboratory, Los Alamos, New Mexico 87545, USA*

(Received 31 October 2006; revised manuscript received 26 March 2007; published 31 May 2007)

We use numerical methods to demonstrate that the phase diagram of $S = 1$ Heisenberg models with uniaxial anisotropy contains an extended supersolid phase. We show that this Hamiltonian is a particular case of a more general and ubiquitous model that describes the low-energy spectrum of some *isotropic* and *frustrated* spin-dimer systems. This result is crucial for finding a spin supersolid state in real magnets.

DOI: 10.1103/PhysRevLett.98.227201 PACS numbers: 75.10.Jm, 75.40.Mg, 75.40.Cx

Theoretical proposals [1] for studying the Bose-Einstein condensation (BEC) with magnetic systems were followed by a vast number of experimental works [2]. These studies were done mainly on spin-dimer compounds. Magnetic systems have the advantage that the magnetic field, which plays the role of the chemical potential, can be varied continuously over a large range of values. A natural question that arises is whether other phases that have been proposed for bosonic gases of atoms can be realized in quantum magnets. The supersolid (SS) state is a prominent and interesting example because the experimental evidence for this novel phase is still inconclusive [3].

The search for the SS phase has motivated the study of different models for hard-core bosons on frustrated lattices [4]. These models are relevant for gases of atoms in a periodic potential. However, the spin $S = 1/2$ Hamiltonians that are obtained from these models by applying a Matsubara-Matsuda transformation [5] are not relevant for real magnetic systems. What makes these models unrealistic for magnetic systems is the large uniaxial exchange anisotropy. Moreover, the longitudinal and the transverse components of the exchange interaction have opposite signs: while the Ising interaction is antiferromagnetic (AFM), the transverse exchange coupling is ferromagnetic. It is then natural and relevant to ask if a SS spin phase can exist in a magnetic system with isotropic (Heisenberg) interactions. In this Letter, we provide an affirmative answer to this question by calculating the quantum phase diagram of an $S = 1$ spin-dimer Heisenberg model. The spin SS phase is induced by the application of a magnetic field whose Zeeman splitting is comparable to the magnitude of the exchange interactions.

To understand the physical origin of the spin SS, we shall start by considering the simplest $S = 1$ Hamiltonian that contains this phase in its phase diagram. This is an $S = 1$-Heisenberg model with uniaxial single-ion and exchange anisotropies on a square lattice:

$$H_H = J\sum_{\langle \mathbf{i},\mathbf{j}\rangle}(S^x_{\mathbf{i}}S^x_{\mathbf{j}} + S^y_{\mathbf{i}}S^y_{\mathbf{j}} + \Delta S^z_{\mathbf{i}}S^z_{\mathbf{j}}) + \sum_{\mathbf{i}}(DS^{z2}_{\mathbf{i}} - BS^z_{\mathbf{i}}), \quad (1)$$

where $\langle \mathbf{i}, \mathbf{j}\rangle$ indicates that $\mathbf{i}$ and $\mathbf{j}$ are nearest neighbor sites, D is the amplitude of the single-ion anisotropy, and Δ determines the magnitude of the exchange uniaxial anisotropy. Note that although the exchange interaction is anisotropic, the longitudinal (J) and transverse (Δ) couplings are both AFM (positive). Henceforth, J is set to unity and all the parameters are expressed in units of J.

The quantum phase diagrams for the spin models considered in this Letter were obtained by using the stochastic series expansion (SSE) quantum Monte Carlo (QMC) method. The simulations were carried out on a square $N = L \times L$ lattice, with $8 \le L \le 16$ and at fixed magnetic field. We find rapid convergence with N for the system sizes studied (see Fig. 1). As the field, B, is varied, the ground state of H_H goes through different phases, including spin-gapped Ising-like (IS) ordered states and gapless XY-ordered (XY) states. The IS phases are characterized by long-range (staggered) diagonal order measured by the longitudinal component of the static structure factor (SSF),

$$S^{zz}(\mathbf{q}) = \frac{1}{N}\sum_{j,k} e^{-i\mathbf{q}\cdot(\mathbf{r}_j - \mathbf{r}_k)}\langle S^z_j S^z_k\rangle. \quad (2)$$

The XY phase has long-range off-diagonal ordering measured by the transverse component of the SSF,

$$S^{+-}(\mathbf{q}) = \frac{1}{N}\sum_{j,k} e^{-i\mathbf{q}\cdot(\mathbf{r}_j - \mathbf{r}_k)}\langle S^+_j S^-_k\rangle. \quad (3)$$

The XY ordering is equivalent to a Bose-Einstein condensation (BEC) whose condensate fraction is equal to $S^{+-}(\mathbf{Q})$, where $\mathbf{Q} = (\pi, \pi)$ is the ordering wave vector. The superfluid density corresponds to the spin stiffness, ρ_s, defined as the response of the system to a twist in the boundary conditions. The stiffness is obtained from the winding numbers of the world lines (W_x and W_y) in the x and y directions: $\rho_s = \langle W_x^2 + W_y^2\rangle/2\beta$.

The IS (XY) phase is marked by a diverging value of $S^{zz}(\mathbf{Q}) \propto N$ [$S^{+-}(\mathbf{Q}) \propto N$] in the thermodynamic limit $N \to \infty$. In addition, ρ_s vanishes in the gapped IS phase while it is finite in the gapless XY phase. A spin SS phase is characterized by a finite value of both $S^{zz}(\mathbf{Q})/N$ *and* ρ_s [6]. Both quantities are always finite for finite-size systems and estimates for $N \to \infty$ are obtained from finite-size scaling.

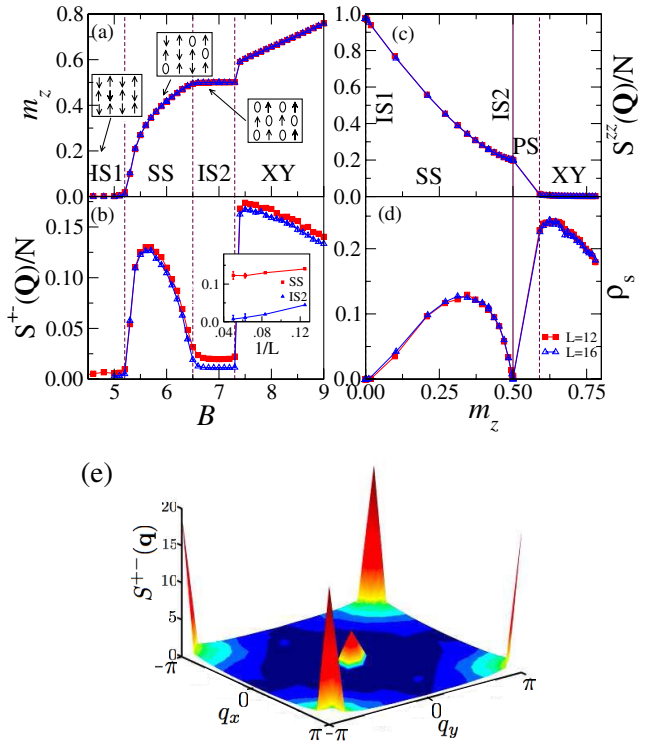

FIG. 1 (color online). Quantum phase diagram of H_H [Eq. (1)] for $D = 1.5$ and $\Delta = 1.8$. (a) Magnetization as a function of field B. The SS phase appears between the two Ising (or solid) orderings denoted by IS1 and IS2. At higher fields, there is a first order transition between the IS2 and the pure XY-AFM phases. (b) Square of the XY-AFM order parameter as a function of B. The inset shows the finite-size scaling of the quantity for two representative points in the SS ($B = 5.7$) and IS2 ($B = 7.0$) phases. (c), (d) Longitudinal component of the staggered SSF and stiffness as a function of the magnetization. In a grand canonical ensemble, no ground state with $0.5 < m_z \lesssim 0.59$ (marked PS) is realized—this corresponds to the discontinuous IS2-XY transition. For a canonical ensemble with magnetization in this range, the ground state phase separates into spatial domains with $m_z = 0.5$ and $m_z \approx 0.59$. (e) Full momentum distribution of the form factor, $S^{+-}(\mathbf{q})$. The peak at $\mathbf{q} = \mathbf{Q}$ in addition to the one at $\mathbf{q} = \mathbf{0}$ indicate that the off-diagonal order is modulated by the presence of simultaneous long-range diagonal order.

Figure 1 shows the quantum phase diagram as a function of magnetic field, B, for $D = 1.5$ and $\Delta = 1.8$. $S^{zz}(\mathbf{Q})$ and ρ_s are plotted as a function of the resulting magnetization m_z. The $m_z(B)$ curve features two prominent plateaus corresponding to different IS phases. For small B, the ground state is a gapped AFM solid (IS1) with no net magnetization. The stiffness, ρ_s, and $S^{+-}(\mathbf{Q})$ vanish in the thermodynamic limit, while $S^{zz}(\mathbf{Q})/N$ is slightly smaller than 1 because the spins are mainly in the $S^z_{\mathbf{i}} = \pm 1$ states depending on to which sublattice they belong. The magnetization stays zero up to the critical field, B_{c1}, that marks a second order BEC quantum phase transition (QPT) to a state with a finite fraction of spins in the $S^z_{\mathbf{i}} = 0$ state. This state has a finite $S^{zz}(\mathbf{Q})/N$ as well as finite ρ_s and $S^{+-}(\mathbf{Q})/N$, i.e., SS order. The diagonal order results from the $S^z_{\mathbf{i}} = \pm 1$ sublattices while the off-diagonal order arises out of a BEC of the flipped spins ($S^z = 0$ "particles"). The magnetization increases continuously up to $B \approx 6.4$, where there is a second BEC-QPT to a second Ising-like state (IS2) where all the $S^z_{\mathbf{i}} = -1$ have been flipped to the $S^z_{\mathbf{i}} = 0$ state. $S^{zz}(\mathbf{Q})/N$ remains divergent for $N \to \infty$, but the stiffness, ρ_s, and condensate fraction, $S^{+-}(\mathbf{Q})$, drop to zero. The ground state remains in the IS2 phase for $6.4 \lesssim B \lesssim 7.2$. Upon further increasing the field, there is a first order transition to a pure XY-AFM phase (m_z changes discontinuously from $m_z = 0.5$ to $m_z \approx 0.59$). In the grand canonical ensemble, no ground state with any intermediate value of the magnetization is realized. For a canonical ensemble with a fixed magnetization $-0.6 < m_z < -0.5$, the ground state will phase separate into IS2 and XY regions with $m_z = 0.5$ and $m_z = 0.59$. In the pure XY phase, the diagonal order vanishes while ρ_s and $S^{+-}(\mathbf{Q})/N$ remain finite. This situation persists until all the spins have flipped to the $S^z_i = 1$ (fully polarized) state.

Further insight into the SS phase is obtained from the momentum dependence of $S^{+-}(\mathbf{q})$ [Fig. 1(e)]. The peaks at $\mathbf{q} = (0, 0)$ and $\mathbf{q} = \mathbf{Q}$ indicate that the off-diagonal long-range order is modulated by the presence of solid order. This confirms that the SF component of the SS phase results from a BEC of $S^z_{\mathbf{i}} = 0$ spin states that occupy the $S^z = -1$ sublattice with higher probability. This feature distinguishes the SS phase from a uniform canted AFM phase.

For smaller values of $\Delta (< D)$, the second magnetization plateau disappears completely (Fig. 2) leaving a second order transition from the SS to the XY phase. The extent of the SS phase decreases with decreasing Δ and vanishes for $\Delta \approx 1$.

We shall now discuss the relevance of these results for finding a SS phase in real magnets. We note that although a U(1) invariant model provides a good description of spin compounds whose anisotropy terms are very small com-

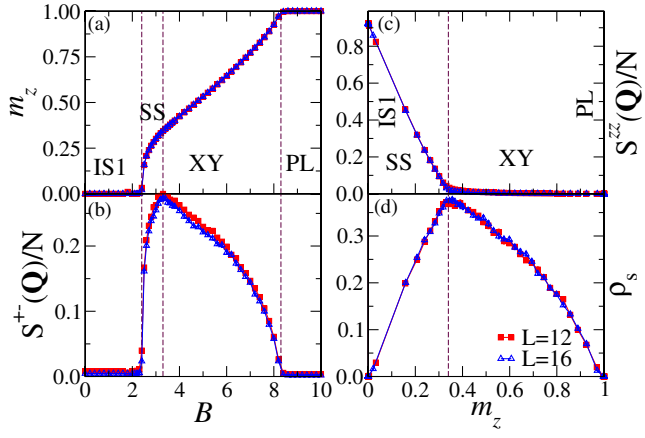

FIG. 2 (color online). Same as Fig. 1, but with parameters $D = 1.5$, $\Delta = 1.2$. The second magnetization plateau disappears completely. Instead, there is a direct (continuous) SS-XY transition. At high fields, there is a transition to a fully polarized state (PL).

pared to the Heisenberg interactions, this invariance is never perfect. The transition metal magnetic ions belong to this class because the spin-orbit interaction is much smaller than the crystal field splitting. These spin systems have small exchange anisotropies for the same reason. Therefore, models that assume opposite signs for J_z and $J_\perp$ [4] or large values of $J_\perp/J_z$ [7] are not directly applicable to these spin compounds. We will show below that it is not necessary to assume a strong uniaxial exchange anisotropy for obtaining a SS phase.

The system to be considered is a square lattice of $S = 1$ dimers (Fig. 3) which only includes *isotropic* (Heisenberg) AFM interactions, an intradimer exchange J_0, and interdimer *frustrated* couplings J_1 and J_2:

$$H_D = J_0 \sum_{\mathbf{i}} \mathbf{S}_{\mathbf{i}+} \cdot \mathbf{S}_{\mathbf{i}-} + J_1 \sum_{\langle \mathbf{i},\mathbf{j}\rangle,\alpha} \mathbf{S}_{\mathbf{i}\alpha} \cdot \mathbf{S}_{\mathbf{j}\alpha} + J_2 \sum_{\langle \mathbf{i},\mathbf{j}\rangle,\alpha} \mathbf{S}_{\mathbf{i}\alpha} \cdot \mathbf{S}_{\mathbf{j}\bar{\alpha}} - B \sum_{\mathbf{i}\alpha} S^z_{\mathbf{i}\alpha}. \quad (4)$$

The index $\alpha = \pm$ denotes the two spins on each dimer. The single dimer spectrum consists of a singlet, a triplet, and a quintuplet (see Fig. 3). The singlet-triplet energy difference is J_0, while the triplet-quintuplet is $2J_0$.

For $J_1, J_2 \ll J_0$, the low-energy subspace of H_D consists of the singlet, the $S^z = 1$ triplet, and the $S^z = 2$ quintuplet (see Fig. 3). The low-energy effective model, H, that results from restricting H_D to this subspace is conveniently expressed in terms of *semi-hard-core* bosonic operators, $g^\dagger_{\mathbf{i}}$ and $g_{\mathbf{i}}$, that satisfy the exclusion condition $g^{\dagger 3}_{\mathbf{i}} = 0$ (no more than two per site) [8,9] and obey the commutation relations of canonical bosons except for the commutator $[g_{\mathbf{i}}, g^\dagger_{\mathbf{j}}] = \delta_{\mathbf{i},\mathbf{j}}(1 - n_{\mathbf{i}})$ ($n_{\mathbf{i}} = g^\dagger_{\mathbf{i}} g_{\mathbf{i}}$ is the number operator). The expression of H in terms of these operators is

$$H = \frac{1}{2}\sum_{\langle \mathbf{i},\mathbf{j}\rangle} (g^\dagger_{\mathbf{i}} g_{\mathbf{j}} + g^\dagger_{\mathbf{j}} g_{\mathbf{i}})(h_1 + h_2 + h_3) - \mu \sum_{\mathbf{i}} n_{\mathbf{i}} + \frac{U}{2}\sum_{\mathbf{i}} n_{\mathbf{i}}(n_{\mathbf{i}} - 1) + V \sum_{\langle \mathbf{i},\mathbf{j}\rangle} (n_{\mathbf{i}} - 1)(n_{\mathbf{j}} - 1) \quad (5)$$

with $h_1 = t_1(n_{\mathbf{ij}} - 2)(n_{\mathbf{ij}} - 3)$, $h_2 = 2t_2(n_{\mathbf{ij}} - 1) \times (3 - n_{\mathbf{ij}})$, $h_3 = t_3(n_{\mathbf{ij}} - 1)(n_{\mathbf{ij}} - 2)$, and $n_{\mathbf{ij}} = n_{\mathbf{i}} + n_{\mathbf{j}}$. The amplitudes t_1, t_2, and t_3 correspond to single-particle hopping terms when there are one, two, or three particles, respectively, on the corresponding bond $\langle \mathbf{i}, \mathbf{j}\rangle$. The case $t_1 = t_2 = t_3 = t$ corresponds to the bosonic Hubbard model with n.n. repulsion [10] in a truncated Hilbert space. Our $S = 1$ Heisenberg Hamiltonian with uniaxial anisotropy, H_H, is obtained for $U = D$, $V = \Delta J$, $\mu = D + B$, and $t_j = \sqrt{2}J/2^{j/2}$ with $j = 1, 2, 3$ after we map on each site the eigenstates of $S^z_{\mathbf{i}}$ onto the eigenstates of $n_{\mathbf{i}}$: $S^z_{\mathbf{i}} = n_{\mathbf{i}} - 1$, and $S^+_{\mathbf{i}} = g^\dagger_{\mathbf{i}}[\sqrt{2} + (1 - \sqrt{2})n_{\mathbf{i}}]$.

As we mentioned before, H also describes the low-energy spectrum of H_D. In this case, we have $U = J_0$, $V = (J_1 + J_2)/2$, $\mu = B - J_0 - z(J_1 + J_2)/2$, and $t_j = 8a^j(J_1 - J_2)/3\sqrt{3}$ with $a = \sqrt{3}/2$, after mapping the eigenstates of $S^z_{\mathbf{i}+} + S^z_{\mathbf{i}-}$ into the eigenstates of $n_{\mathbf{i}}$ by the simple relations: $n_{\mathbf{i}} = S^z_{\mathbf{i}+} + S^z_{\mathbf{i}-}$ (see Fig. 3) and $g^\dagger_{\mathbf{i}} = \frac{1}{\sqrt{2}}(S^+_{\mathbf{i}+} - S^+_{\mathbf{i}-})[\frac{\sqrt{3}}{2\sqrt{2}} + (1 - \frac{\sqrt{3}}{2\sqrt{2}})S^z_{\mathbf{i}}]$. Figure 4 shows the quantum phase diagram as a function of μ (or B) for $U = 30.0$ and $V = 7.0$ [$(J_1 - J_2)/2$ is the unit of energy]. This set of parameters corresponds to $J_0 = 30$, $J_1 = 8$, and $J_2 = 6$ that satisfies the conditions $J_0 > z(J_1 + J_2)/2$ and $J_0 \gg z(J_1 - J_2)/2$ necessary for the validity of H as a low-energy effective model for H_D.

At small μ or B, the empty state (all the dimers in a singlet state) has the lowest energy. For $\mu > \mu_{c1}$ ($B > B_{c1}$) a finite density of bosons (triplets) is stabilized in the ground state giving rise to a BEC (XY-AFM ordering) at $T = 0$ with a finite the stiffness ρ_s. The absence of solid (Ising) ordering is indicated by $S^{zz}(\mathbf{Q})/N \to 0$. The density (magnetization) increases monotonically as a function of μ

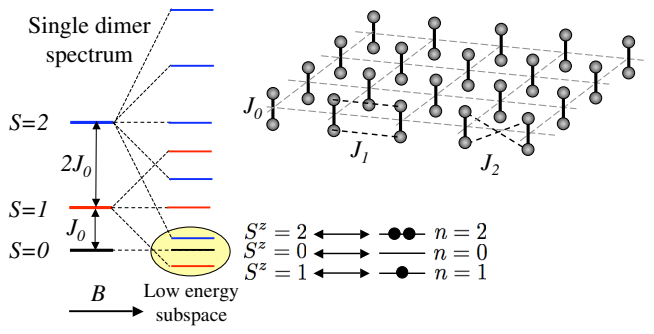

FIG. 3 (color online). Square lattice of $S = 1$ dimers with an intradimer Heisenberg AFM interaction J_0 and interdimer interactions J_1 and J_2. The left side shows the low-energy subspace of the single dimer spectrum in the presence of a magnetic field.

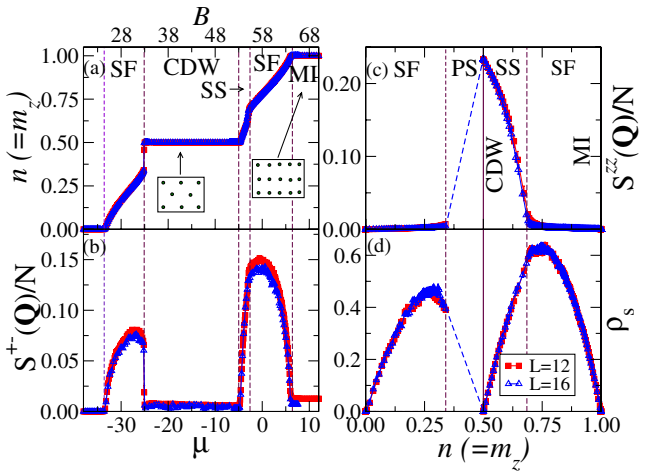

FIG. 4 (color online). Quantum phase diagram of H (5) for $U = 30.0$, $V = 7.0$. (a) Particle density n or m_z as a function of the chemical potential μ (lower axis) or field B (upper axis). (b) Condensate fraction or square of the AFM-XY order parameter. (c), (d) The staggered SSF and stiffness as a function of $n = m_z$. The range of densities marked PS is inaccessible in the grand canonical ensemble and would result in a phase separated state in a canonical ensemble.

or B until $\mu = \mu_{c2} \approx 2.9$, where there is a discontinuous transition to a charge-density wave (CDW) or Ising-like phase with $n = m_z = 0.5$ (the dimers of one sublattice are in a triplet state while the other dimers remain in the singlet state). For $\mu > \mu_{c3} \sim 23.4$, some of the dimers of the singlet sublattice are turned into triplets that propagate primarily on the singlet sublattice ($U \gtrsim zV$ where $z = 4$ is the coordination number). Consequently, there is a BEC-QPT [broken U(1) symmetry under rotations around the z axis] in $\mathcal{D} = d + 2$ dimensions to a SS phase, where d is the spatial dimensionality. The diagonal or solid order disappears at an Ising-like quantum critical point in $\mathcal{D} = d + 1$ dimensions for $\mu = \mu_{c4} \approx 25.4$ (broken Z_2 symmetry of translation by one lattice parameter followed by a π rotation around the z axis). Upon further increase in μ, the filling increases monotonically in the resulting SF phase until the ground state enters a Mott insulating (MI) phase with all the dimers in the triplet state.

The mechanism for the formation of the SS phase is explained most readily in the bosonic language [10]. In the strong coupling limit (U, $V \gg t$), the half-filled ground state ($n = \frac{1}{2}$) is a checkerboard solid (one sublattice is single occupied while the other sublattice is empty). Doping away from $n = \frac{1}{2}$ results in different scenarios depending on the nature of doping and the relation between the coupling constants U and V. *Extracting* bosons from the $n = 1/2$ crystal costs chemical potential μ but no potential energy. The kinetic energy gain of the resulting holes is quadratic in t for isolated holes [$\mathcal{O}(t^2/V)$], but becomes *linear* in t if the holes segregate in a SF bubble. Consequently, if the total density is fixed, the system separates in a commensurate crystal with $n = 1/2$ and a uniform SF region with $n < 1/2$. This implies a first order transition between the solid and the SF phases as a function of μ (see Figs. 1 and 4).

Doping of the $n = 1/2$ crystal with *additional* bosons works differently depending on the relation between V and U. The energy cost to place a boson at an empty (occupied) site is $E_0 \equiv zV - \mu$ ($E_1 \equiv U - \mu$). Respectively, for $U \gg zV$, the additional bosons fill empty sites and mask the checkerboard modulation; for $U - zV \gg |t|$ the situation is precisely particle-hole conjugate to hole doping. In particular, in the hard-core limit $U \to \infty$, the crystalline order is always unstable for $n \neq 1/2$. However, for $zV \sim U$, the bosons can be placed on either an occupied or unoccupied site. The kinetic energy gain of the added boson is now linear in t because the potential barrier, $|zV - U|$, for moving the bosons to nearest neighbors is not much bigger than t. As a result, the added bosons form a SF phase on top of the density wave background and hence the ground state has simultaneous solid and SF orders. This SS phase is stable for a sufficiently small concentration of added bosons. This is confirmed by the quantum phase diagram shown in Fig. 4 where the SS phase appears right next to the $n = 1/2$ CDW. We emphasize that this phase requires to have two bosons on the same site, which is not possible for hard-core bosons (or, equivalently, for $S = \frac{1}{2}$ spins).

Finally, we note that the hopping term of H becomes negative for $J_2 > J_1$. If we now consider the Hamiltonian H_D for a triangular lattice of $S = 1/2$ dimers (instead of a square lattice $S = 1$ dimers) in the limit $J_0 \ll J_1$, J_2, the resulting low-energy effective model is a $t - V$ Hamiltonian for hard-core bosons on a triangular lattice, where $t = (J_1 - J_2)/2$, $V = (J_1 + J_2)/2$, and $\mu = -J_0 + B$. This model contains a SS phase in its quantum phase diagram for $t < 0$ and $V \gg |t|$ [4], which implies that the triangular lattice of $S = 1/2$ (or $S = 1$) dimers with frustrated (J_1 and J_2) interdimer couplings provides an alternative realization of a spin SS.

In summary, we have shown that simple two-dimensional $S = 1$ Heisenberg models have a spin SS ground state induced by magnetic field. The physical mechanism that leads to this phase does not depend on the dimensionality and similar results are expected for three- and one-dimensional lattices [11,12]. These results provide the required guidance for finding this novel phase in real spin systems. The crucial ingredients for the described mechanism are *dimerized* spin structures and *frustrated* interdimer couplings.

LANL is supported by US DOE under Contract No. W-7405-ENG-36.

[1] I. Affleck, Phys. Rev. B **41**, 6697 (1990); T. Giamarchi and A. M. Tsvelik, Phys. Rev. B **59**, 11 398 (1999); T. M. Rice, Science **298**, 760 (2002).
[2] N. Cavadini *et al.*, Phys. Rev. B **65**, 132415 (2002); A. Oosawa *et al.*, Phys. Rev. B **66**, 104405 (2002); Ch. Ruegg *et al.*, Nature (London) **423**, 62 (2003); M. Jaime *et al.*, Phys. Rev. Lett. **93**, 087203 (2004); S. Sebastian *et al.*, Nature (London) **441**, 617 (2006).
[3] E. Kim and M. H. W. Chan, Nature (London) **427**, 225 (2004); Science **305**, 1941 (2004).
[4] M. Boninsegni and N. Prokof'ev, Phys. Rev. Lett. **95**, 237204 (2005); S. Wessel and M. Troyer, Phys. Rev. Lett. **95**, 127205 (2005); D. Heidarian and K. Damle *ibid.* **95**, 127206 (2005); R. G. Melko *et al.*, *ibid.* **95**, 127207 (2005).
[5] T. Matsubara and H. Matsuda, Prog. Theor. Phys. **16**, 569 (1956).
[6] Spin-orbit interactions will remove the finite stiffness in real systems by opening a gap in the excitation spectrum. However, an idealized U(1)-invariant model describes most of the properties of some real magnets to a very good approximation.
[7] K.-K. Ng and T. K. Lee, Phys. Rev. Lett. **97**, 127204 (2006); N. Laflorencie and F. Mila, cond-mat/0702249.
[8] C. D. Batista and G. Ortiz, Phys. Rev. Lett. **86**, 1082 (2001).
[9] C. D. Batista and G. Ortiz, Adv. Phys. **53**, 1 (2004).
[10] P. Sengupta *et al.*, Phys. Rev. Lett. **94**, 207202 (2005).
[11] G. G. Batrouni, F. Hébert, and R. T. Scalettar, Phys. Rev. Lett. **97**, 087209 (2006).
[12] P. Sengupta and C. D. Batista (to be published).